Performance of the Partition of Unity Finite Element Method for the modeling of Timoshenko beams

T. Zhou, J.-D. Chazot, E. Perrey-Debain, L. Cheng

Version of Record: https://www.sciencedirect.com/science/article/pii/S0045794919303098
Manuscript_b6c7c8d75403a955b5544006450a6e8c

Performance of the Partition of Unity Finite Element Method for the modeling of Timoshenko beams

T. Zhou[a], J.-D. Chazot[b], E. Perrey-Debain[b], L. Cheng[a,*]

[a]*Department of Mechanical Engineering, The Hong Kong Polytechnic University, Hong Kong, P. R. China*
[b]*Laboratoire Roberval, FRE UTC-CNRS 2012, Université de Technologie de Compiègne 60205 Compiègne BP 20529 France*

Abstract

The partition of unity finite element method (PUFEM) is developed and applied to compute the vibrational response of a Timoshenko beam subject to a uniformly distributed harmonic loading. In the proposed method, classical finite elements are enriched with three types of special functions: propagating and evanescent wave functions, a Fourier-type series and a polynomial enrichment. Different formulations are first assessed through comparisons on the frequency response functions at a specific point on the beam. The computational performance, in terms of both accuracy and data reduction, is then illustrated through convergence analyses. It is found that, by using a very limited number of degrees of freedom, the wave enrichment offers highly accurate results with a convergence rate which is much higher than other formulations. Evanescent waves and the constant term in the wave basis are also shown to play an important role. In all cases, the proposed PUFEM formulations clearly outperform classical finite element method in terms of computational efficiency.

Keywords: Partition of Unity Finite Element Method, Timoshenko beam, Wave propagation, Lagrange multiplier
PACS:

1. Introduction

The numerical simulation of mechanical waves in the so-called mid-frequency range has been the subject of intensive research in the past two decades and continues to be a very challenging topic for many research engineers and applied mathematicians (see [1], [2] and [3]). This mid-frequency gap in modelling capabilities separates the low frequency range for which standard Finite Element Method (FEM) are applicable and largely used and the high-frequency range which is normally dealt with by statistical methods such as the very popular Statistical Energy Analysis (SEA). To better tackle short-wave simulation problems, enriched methods have been developed in recent decades. These numerical techniques have been tailored to incorporate a *prior* knowledge of the propagating waves in the formulation. A rather complete survey on the topic can be found in a recent review paper [4]. Among these methods the Partition of Unity Finite Element Method (PUFEM) has the advantage of possessing high similarities with the classical FEM (see Refs. [5, 6]). It can be easily implemented for numerical analysis using the existing finite element meshes and simulation codes. The PUFEM has been applied to simulate

*Corresponding authors
Email addresses: jean-daniel.chazot@utc.fr (J.-D. Chazot), li.cheng@polyu.edu.hk (L. Cheng)

the acoustic and elastic wave propagation (see Refs. [7, 8, 9] and Refs. [10, 11] respectively). In particular, numerical simulations of acoustic waves propagating in air, porous and poro-elastic media [12, 13, 14] have also been attempted in our previous work, which constitutes a natural extension of the method for noise control applications.

Up to now, there are few works on the modelling of vibrations of beams and plates with the PUFEM. The first paper relating to this topic is probably the static analysis of Timoshenko beams with elastic supports presented by Babuska in Ref. [15], which shows that shear locking disappears with PUFEM enrichments, contrary to classical FEM. Vibrational modes of a cantilever beam have been studied independantly by Arndt *et al.* [16, 17] and Shang-Hsu [18] with an enrichment based on trigonometric sine expansions, hierarchical polynomial functions and modal expansion (this latter is based on an idea presented by Craig [19]). This type of enrichment, though failing to capture the essential wave characters of the solution, except maybe for the modal expansion which somehow contains the geometry and material properties of the beam in the formulation, has the advantage of being frequency-independent thus allowing the use of standard algebraic modal analysis solvers. Polynomial functions in PUFEM have also been used to the development of enriched Mindlin plate elements [20] and in this context, the method shares similarities with p-FEM technique. De Bel et al. [21] used flexural waves propagating in different directions as the enrichment functions. The originality of the approach is that the propagation angle is generated iteratively at each node of the PUFEM mesh. However, shear deformations and rotary inertia effects are neglected in their analysis. Finally, though the method does not formally fit in with the PUFEM approach, we can cite the early work of Hashemi et al. [22] who developed a Dynamic Finite Element for the vibrational analysis of spinning beams, by including frequency dependent trigonometric shape functions in their formulation.

Motivated by the above analyses, the aim of this paper is to develop and investigate the applicability of PUFEM to the dynamic analysis of thin vibrating structures. To this end, a simply supported beam under a distributed harmonic loading is chosen as a benchmark for further developments involving vibro-acoustic coupling in one and two dimensions. Timoshenko beam theory is adopted to ensure a correct description of the vibration behaviour at high frequencies, when the wavelength is comparable to the thickness of the beam. Furthermore, as opposed to the classical fourth-order wave equation of the Euler-Bernoulli beam whose numerical treatment requires the use of specific C^1 elements [17], Timoshenko theory leads to a coupled system of second order partial differential equations for the translational and rotational displacements which permits to employ conventional piecewise-continuous Lagrangian finite element shape functions for the partition of unity. As one of the key ingredients of the method, particular attention is paid to choosing an appropriate function space for the finite element enrichment, which should have good approximation properties for the solutions to a given differential equation [5]. In the present work, exact solutions of an unloaded infinite beam including both the propagating and evanescent waves [23] are exploited, with the addition of additional terms to account for the pressure loading. Comparisons are made with classical type of enrichments such as Fourier-type series and polynomials. Finally, the treatment of the boundary conditions needs particulate attention. Although classical finite element procedures can be followed for some particular types of enrichment functions, penalty or Lagrange's multiplier technique [21, 17] is adopted to accommodate all types of enrichment functions. Numerical analyses are conducted with comparisons among different types of enrichment functions, in terms of computational accuracy and data reduction. It is concluded that the wave basis in the PUFEM is the best approach leading to the best convergence rate.

The paper is organized as follows. After recalling the classical Timoshenko beam theory as well as its associated variational formulation in Section 2, PUFEM Timoshenko beam ele-

ments, with three type of enrichments, are constructed and explained in Section 3. In Section 4, classical FEM formulations including linear elements with exact and reduced integration and an enhanced formulation based on a cubic and quadratic interpolation for the transverse displacement and the rotation are presented. This should serve as a reference solution and allows to identify, wherever necessary, shear-locking effects. In the last section, performance of PUFEM elements is shown and compared with classical FEM. In all cases, a reference solution, is obtained using linear interpolation calculated on a very refined mesh. Convergence curves, corresponding to h-refinement', i.e. by reducing the element size, and 'p-refinement', i.e. by increasing the number of enrichment functions, are given and analyzed. The role of evanescent waves in the PUFEM wave basis is also discussed.

2. Timoshenko beam theory

The flexural vibration of beams is under investigation. Figure 1 presents a schematic representation associated with the two main theories dedicated to beams: Euler-Bernoulli and Timoshenko theories. For the latter the displacements of the beam are denoted by $u(x,z) = z\beta(x)$

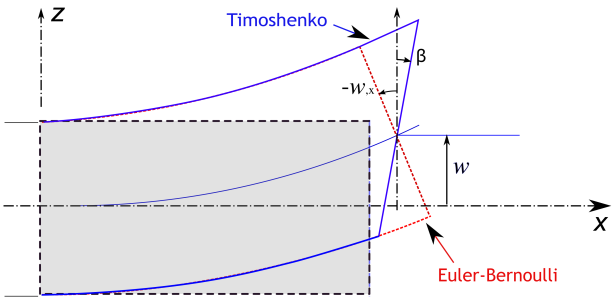

Figure 1: Beam description in the x-z plane.

and $w(x,z) = w(x)$ where β is the total angle of rotation of the section, and w is the displacement of the mid-surface in the z-direction. These two independant variables obey the equations of motion:

$$f_z + \kappa G S \gamma_{,x} = \rho S \ddot{w}, \tag{1}$$

$$EI\beta_{,xx} - \kappa G S \gamma = \rho I \ddot{\beta}, \tag{2}$$

where $\gamma = \beta + w_{,x}$ is the shear deformation angle and f_z is the distributed load. The material properties are the Young's modulus E, the shear modulus G and the density ρ. The geometrical parameters are the shear correction factor $\kappa = 5/6$, the second moment of area I, the cross section area S and the beam length L. With simply supported boundary conditions, the displacement and the bending moment vanish at the locations of the two supports , i.e. at $x = 0, L$. In this case, the associated variational formulation writes

$$\int_0^L \left(\delta w \rho S \ddot{w} + \delta\beta \rho I \ddot{\beta} + \delta\beta_{,x} EI\beta_{,x} + \delta\gamma \kappa G S \gamma - \delta w f_z \right) \mathrm{d}x - \delta w_0 \lambda_0 - \delta w_L \lambda_L = 0, \tag{3}$$

where $\delta(\cdot)$ donates the virtual quantity and w_0 and w_L are the displacement at $x = 0, L$, respectively. In formulation (3), the transverse shear forces appear naturally as Lagrange multipliers

λ_0 and λ_L. Though it is common to discard these terms by simply choosing $\delta w_0 = \delta w_L = 0$, the best way to handle the boundary terms with PUFEM is to weakly enforce the essential conditions as:

$$\delta\lambda_0 w_0 = \delta\lambda_L w_L = 0, \qquad \forall(\delta\lambda_0, \delta\lambda_L). \tag{4}$$

This has the advantage of preserving the symmetry of the linear sytem and permits to handle efficiently the coupling conditions between two media (see for instance [9, 12, 13]).

3. Application of the PUFEM

In this work, we only investigate the Timoshenko beam vibration subject to a harmonic loading at an angular frequency ω and the time-dependent term $e^{-i\omega t}$ is omitted hereafter. As done in classical FEM, the beam is partitioned into non-overlapping elements and the degrees of freedom are interpolated over each elements with nodal unknowns. The key ingredient of the PUFEM relies on the enrichment of the conventional finite element approximation by including special functions in order to enhance the convergence of the numerical solution. For an infinite beam, the two propagating and two evanescent waves characterized by the wavenumbers write (see Ref. [23] for more details):

$$k_p = \sqrt{\frac{\rho I\omega^2(1 + E/(\kappa G)) + \sqrt{\delta}}{2EI}}\,, \tag{5}$$

$$k_e = \sqrt{\frac{-\rho I\omega^2(1 + E/(\kappa G)) + \sqrt{\delta}}{2EI}}\,, \tag{6}$$

with $\delta = (\rho I\omega^2)^2(1 - E/(\kappa G))^2 + 4EI\rho S\omega^2$. Each PUFEM element of length $l_e = x_2 - x_1$ is given by the geometric mapping $x(\xi) = N_1 x_1 + N_2 x_2$ where x_i are the nodes and ξ is the coordinate in the reference frame $\xi \in [0, 1]$. Here, $N_1 = \xi$ and $N_2 = 1 - \xi$ are the classical linear shape functions. The transverse displacement and the rotation are then expanded as:

$$w = \sum_{i=1}^{2} N_i(\xi) \sum_{n=1}^{N} A_i^n \, \Psi_i^n, \tag{7}$$

$$\beta = \sum_{i=1}^{2} N_i(\xi) \sum_{n=1}^{N} B_i^n \, \Psi_i^n. \tag{8}$$

For wave enrichment, we consider $N = 5$ functions Ψ_i^n defined as:

$$\Psi_i^n \in \{1, \cos[k_p(x - x_i)], \sin[k_p(x - x_i)], \cosh[k_e(x - x_i)], \sinh[k_e(x - x_i))]\}, \tag{9}$$

where the constant term $\Psi_i^1 = 1$ has been added in the enrichment in order to capture contributions of the distributed load, i.e. the particular solutions of the governing equations [24]. Two other kinds of enrichment are also considered in the present work. The first one is a polynomial enrichment:

$$\Psi_i^n \in \{1, \eta_i, {\eta_i}^2, {\eta_i}^3, {\eta_i}^4, \ldots\}\,, \tag{10}$$

where $\eta_i = (x - x_i)/l_e$. For $N = 2$, there are four enrichment terms associated with one polynomial-enriched element whilst the highest order of the corresponding bases (7) and (8) is

two. Therefore, these basis functions are linearly dependent since only three polynomial terms form a complete quadratic basis. The second one is a Fourier-type series

$$\Psi_i^n \in \{1, \cos(\pi\eta_i), \sin(\pi\eta_i), \cos(2\pi\eta_i), \sin(2\pi\eta_i), \ldots\} \ . \tag{11}$$

Note that (i) Fourier and polynomial enrichments can be built with an arbitrary order N whereas, by construction, the wave enrichment is necessarily limited to $N = 5$. (ii) Since the PUFEM element can contain many wavelengths, the elementary mass and stiffness matrices associated with the PUFEM expansion (7) and (8) must be constructed using sufficient Gaussian integration points in order to ensure convergence.

4. Classical FEM

In order to evaluate the PUFEM efficiency in comparisons with classical FEM formulations, two beam finite elements are reminded here: a linear element used as a reference, and an enhanced element which is also commonly used.

4.1. Linear element

The beam is discretized with linear shape functions:

$$w = \sum_{i=1}^{2} A_i \, N_i(\xi) \quad \text{and} \quad \beta = \sum_{i=1}^{2} B_i \, N_i(\xi). \tag{12}$$

The associated elementary stiffness matrix can be evaluated with exact integration method. However, this formulation over-emphases the effect of shear deformation in comparison with the bending effect, which would generate shear-locking effects for the cases where the Euler-Bernoulli or thin beam model is applicable. To tackle the problem, a reduced integration technique is usually employed [25, 26, 27]. The linear element with reduced integration serves as a reference solution and permits to identify, wherever needed, the shear-locking effects. Details of linear elements using reduced and exact integration schemes are given in the Appendix.

4.2. Enhanced element

A specific timoshenko beam element is also often encountered in the litterature (see Refs. [28, 29, 26]). This enhanced element is also tested in this work, and compared with the PUFEM. It is based on a cubic and a quadratic interpolation for the transverse displacement w and the rotation β, respectively, with an added constraint between w and β in order to satisfy the static equilibrium equation. This type of enhanced element is also free of shear locking. The displacement and rotation are expanded as

$$w = \sum_{i=1}^{4} C_i \, \hat{N}_i(\xi) \quad \text{and} \quad \beta = \sum_{i=5}^{8} C_i \, \hat{N}_i(\xi), \tag{13}$$

where $\hat{N}_i(\xi)$ is the shape function of the enhanced element and the Appendix gives their detailed expressions.

Geometrical parameters	Material parameters
$L = 1$ m	$E = 70$ GPa
$h = 0.01$ m	$\rho = 2780$ kg/m^3
$b = 0.01$ m	$G = 27$ GPa

Table 1: Parameters used in our computations.

5. PUFEM performance

The tested configuration is a simply supported beam subject to a uniformly distributed harmonic loading with a unit amplitude. The geometrical and material parameters of the beam are tabulated in Table 1.

The performance of the PUFEM with different enrichment functions is evaluated through the comparisons of their Frequency Response Function (FRF), as shown in Figure 2. The reference solution is obtained using classical linear elements with reduced integration and with 50'000 elements (in grey). The calculations of the FRF curves with PUFEM using different enrichment methods, i.e. wave enrichment, Fourier and polynomial enrichment, are all carried out using 2 elements and 5 enrichment functions ($N = 5$) which corresponds to a total number of degrees of freedom of $3 \times 2 \times 5 = 30$. It can be seen from Figure 2 that PUFEM can provide accurate predictions up to a certain frequency limit, depending on the enrichment function. Clearly, the wave enrichment (blue solid line) offers best performance and a good agreement with the reference solution up to 3000 Hz, above which small, but growing, discrepancies start to appear. The other two enrichments, using the Fourier series (green dotted line) and the polynomial functions (red mixed line), are only accurate up to a reduced frequency range, around 1400 and 500 Hz, respectively. Of course, the frequency band can be extended by applying either a h-refinement or a p-refinement, as evidenced by the following convergence analyses. Figure 3 shows the deformed shape along the beam close to the upper limit frequency for each enrichment. It can be seen that the PUFEM with waves can capture multiple wavelenghs per element (up to 3 for the present case), which is a typical feature of wave enriched elements.

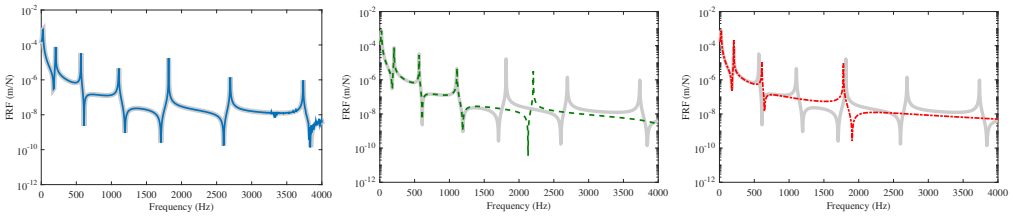

Figure 2: FRF comparison w_o/F_e (at $L/4$ from left end): reference solution with classical FEM, PUFEM with the wave enrichment, PUFEM with the Fourier enrichment, PUFEM with the polynomial enrichment.

Figure 4 compares the convergence of the different formulations obtained using a h-refinement for two specific frequencies: 1000 and 3500 Hz while keeping the same enrichment order ($N = 5$) with PUFEM. The L^2 errors are plotted versus the number of degrees of freedom N_{dof}. Here, errors are estimated via L^2-norm as

$$\varepsilon = \frac{\sqrt{\int_0^L |w_{computed} - w_{ref}|^2 \mathrm{d}x}}{\sqrt{\int_0^L |w_{ref}|^2 \mathrm{d}x}} \times 100\% \,, \tag{14}$$

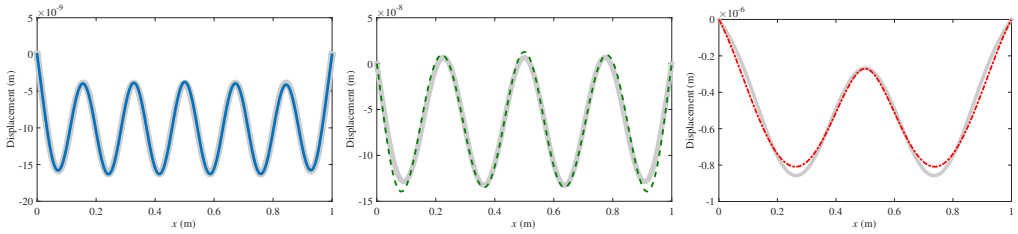

Figure 3: Illustration of the deformed shape at 3000Hz, 1200Hz and 400Hz from left to right. ▬ reference solution with classical FEM, —— PUFEM with the wave enrichment, – – – PUFEM with Fourier enrichment, – · – PUFEM with polynomial enrichment.

where w_{ref} is the reference solution. The superiority of the PUFEM with wave enrichment can be clearly seen: the highest convergence rate and very good accuracy with a very small number of degrees of freedom even at high frequencies. It should be noted that the error is limited here by the accuracy of the reference solution. This explains the visible plateau by the wave enrichment at a very low error level (around $10^{-5}\%$ for 1000Hz and $10^{-4}\%$ for 3500Hz). The PUFEM with the polynomial enrichment is also very efficient with a high convergence rate. Indeed, results indicate that the error behaves like $\varepsilon \sim C l_e^{\alpha}$ where $\alpha \approx 8$ (recall that l_e is the element length and the total number of degrees of freedom N_{dof} is inversely proportional to l_e). The convergence law of the classical FEM with complete polynomial expansions does not apply to the PUFEM with polynomial enrichment. It is remarkable to see that classical linear elements, with and without reduced integration, as well as the enhanced element formulation give the same convergence rate and $\varepsilon \sim C' l_e^2$, which is line with the classical linear interpolation. What differentiates the three formulations is that (i) results obtained with the enhanced element are 100 times more accurate than the linear formulation with reduced integration and (ii) classical linear FEM with exact integration suffers from slow convergence due to shear-locking effects which can be avoided at the expense of a very refined mesh. Finally, the Fourier-type enrichment performs similarily to classical FEM once the length of the element is sufficiently small, this is because the mesh spacing is decreased and the oscillating nature of the solution within a single element is lost and the Fourier series, with a fixed order of approximation (here $N = 5$), does not show any advantage with respect to classical FEM [30]. The fact that the exact solution has a strong wave component with wavenumber $k_p = 2\pi/\lambda_p$ explains the peculiar behaviour clearly observed when finite elements are larger. Since the Fourier enrichment is chosen to capture half of a wavelength up to one wavelength per element, the formulation is expected to yield best results around $0.5 \leq l_e/\lambda_p \leq 1$ and this is confirmed in Table 2 where numerical errors are shown with respect to that criteria. Finally, none of the PUFEM formulations suffers from shear-locking and this is consistent with observations made in Ref. [18].

As mentioned before, a p-refinement analysis is possible with Fourier and polynomial enrichments. Results are shown in Figure 5 for two selected frequencies, 1000 and 3500 Hz. For the sake of comparison, the previous results using h-refinement are also reported. In the present case, the beam is meshed with 2 elements (same as in Figure 2 and 3) while the approximation order N is increased. As expected, p-refinement performs better than h-refinement does. The Fourier enrichment behaves nearly as well as the wave enrichment. However, if the polynomial shows similar trends for low and moderate appproximation order N, results quickly deteriorate as soon as the exponent in the polynomial exceeds a certain value. The reason for this probably stems from the linear dependence and the loss of orthogonality properties of the polynomial bases, and the occurrence of very ill-conditioned matrices [20]. In an attempt to clarify this, the

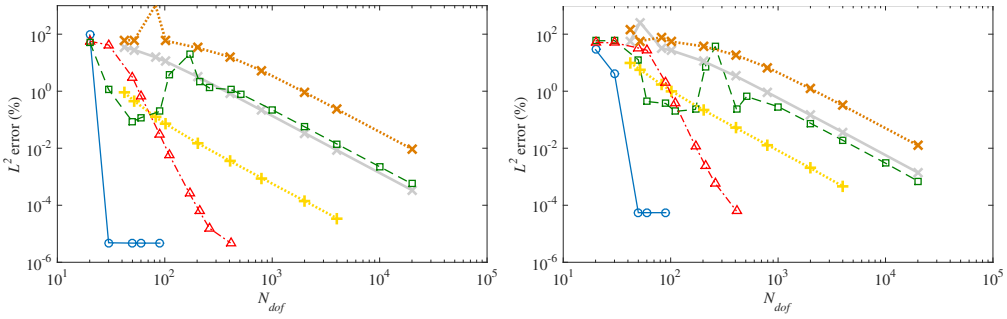

Figure 4: Convergence curves obtained with a h-refinement at 1000Hz (left) and 3500Hz (right). —×— classical FEM, - - -×- - - linear FEM with exact integration, - - -+- - - enhanced FEM, —◯— PUFEM with wave enrichment, – □ – PUFEM with Fourier enrichment, – -△- – PUFEM with polynomial enrichment.

	1000Hz		3500Hz	
N_{dof}	l_e/λ_p	ε (%)	l_e/λ_p	ε (%)
20	3.33	53.38	6.28	58.45
30	1.66	1.14	3.14	59.69
50	**0.83**	**0.08**	1.57	12.58
60	**0.66**	**0.11**	**1.25**	**0.43**
90	**0.41**	**0.19**	**0.78**	**0.37**
110	0.33	3.83	**0.62**	**0.19**
170	0.20	19.97	**0.39**	**0.22**
210	0.16	2.11	0.31	7.29
260	0.13	1.30	0.25	36.68
410	0.08	1.14	0.15	0.23
510	0.06	0.80	0.12	0.64
1010	0.03	0.21	0.06	0.28
...	...	...	...	...

Table 2: Convergenve of Fourier-type enrichment (corresponding to – □ – in Figure 4) (in bold are values below 0.5% at the cup).

associated conditioning numbers of the system matrices are shown in Figure 6. As opposed to classical FEM, PUFEM formulations clearly produce matrices with a higher condition number, a well-known feature which is inherent to the method [20]. This, however, does not necessarily impede on the quality of the results (some explanations are given by one of the present authors in [31] in a BEM context). For instance, wave and Fourier enrichments show very good stability despite a growing condition number wich is comparable, though smaller, with that of the polynomial enrichment. An alternative would be to employ orthogonal polynomials instead, in which case the method would share some similarities with hierachical FEM [32].

Since the wave enrichement offers best performance. It is relevant to assess the influence of each term in the wave basis Figure 7 shows the convergence at 1000 Hz and 3500 Hz using h-refinement with the complete wave basis, and the one with certain terms removed, in comparison with the classical linear FEM results. When the constant term is removed from the wave bais, i.e. $\Psi_i^1 = 1$, the PUFEM is only enriched with free vibration solutions. With a uniform loading, this has noticeable effects on the convergence rate and on the number of degrees of freedom required to produce accurate results. When the evanescent waves are removed, the nearfield

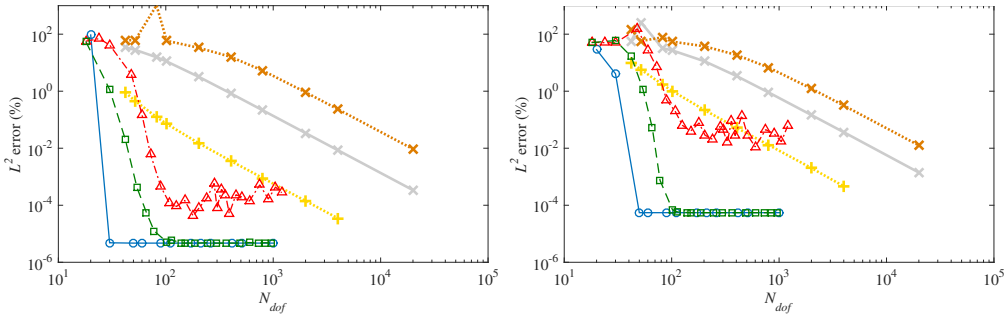

Figure 5: Comparison of convergence at 1000Hz (left) and 3500Hz (right). —×— h-refinement with classical FEM, ---×--- h-refinement with linear FEM and exact integration, ---+--- h-refinement with enhanced FEM, —○— h-refinement for PUFEM with wave enrichment, – □ – p-refinement for PUFEM with Fourier enrichment, – - △ – - p-refinement for PUFEM with polynomial enrichment.

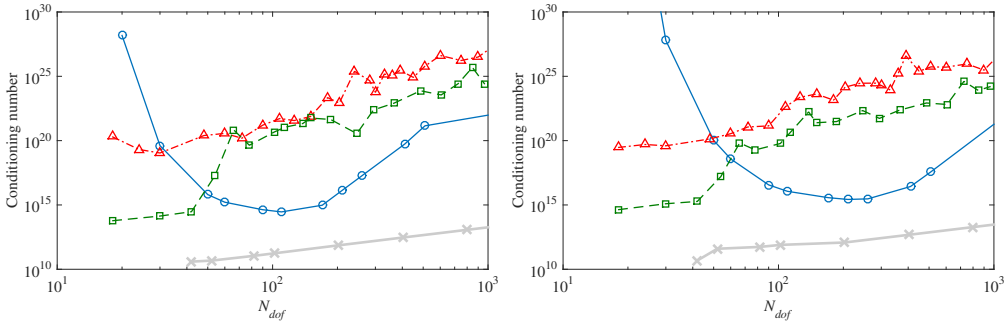

Figure 6: Comparison of conditioning number with h and p refinement at 1000Hz on the left and 3500Hz on the right. —×— h-refinement for classical FEM, —○— h-refinement for PUFEM with wave enrichment, – □ – p-refinement for PUFEM with Fourier enrichment, – - △ – - p-refinement for PUFEM with polynomial enrichment.

effects of the decaying waves near the beam supports cannot be properly modelled and this, again, has noticeable effects on the convergence rate. In all scenarios, however, all PUFEM formulations clearly outperforms classical FEM to various extent.

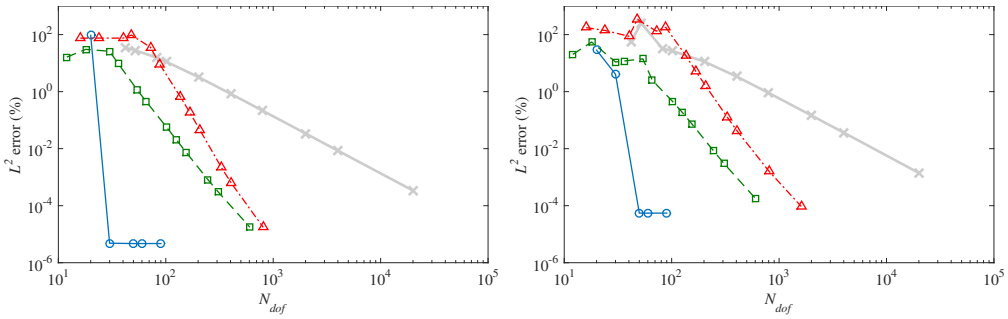

Figure 7: Convergence curves obtained with h-refinement at 1000Hz on the left and 3500Hz on the right. —×— Linear FEM with reduced integrations, —○— PUFEM with complete wave enrichment, – - △ – - PUFEM wave enrichment without the constant term, – □ – PUFEM wave enrichment without the envanescent waves.

6. Conclusions

In this study, PUFEM Timoshenko beam elements are developed for solving forced vibration problems. Three types of enrichment are investigated: the wave enrichment based on the solutions of the governing equations, Fourier series and the polynomials. The performance of different enrichment functions is numerically evaluated in terms of frequency response functions and convergence properties.

Analyses lead to the prevailing conclusion that the wave enrichment, through the embodiment of specific information based on physical features, offers the best performance in terms of both computational accuracy and data reduction. In all cases, all three PUFEM formulations outperform the classical finite element discretization and the best convergence is obtained using a p-refinement strategy. However, it is found that, due to a lack of orthogonality property, the polynomial basis is recommended to adopt a h-refinement strategy instead. Finally, the constant term in the wave basis shows its importance to account for the loading effects.

As a final remark, one direction of particular interest is to further extend the method to the numerical prediction of complex vibrating structures involving vibro-acoustic coupling. In this regard, it would be interesting to analyse more specifically the type of enrichment needed to correctly capture the spatially oscillating pattern of the loading due to surface acoustic waves.

7. References

[1] W. Desmet, B. Pluymers, and O. Atak. Final report summary - mid-frequency. *CAE Methodologies for Mid-Frequency Analysis in Vibration and Acoustics*, 2012.

[2] EPSRC funded workshop. Boundary and finite element methods for high frequency scattering problems. Department of Mathematics and Statistics, University of Reading, 2014.

[3] G. Tanner and B. Mace. Special issue of wave motion - "innovations in wave modelling". *Wave Motion*, 4(51):547–684, 2014.

[4] E. Deckers, O. Atak, L. Coox, R. DAmico, H. Devriendt, S. Jonckheere, K. Koo, B. Pluymers, D. Vandepitte, and W. Desmet. The wave based method: An overview of 15 years of research. *Wave Motion*, 51(4):550–565, 2014.

[5] J.M. Melenk and I. Babuška. The partition of unity finite element method: Basic theory and applications. *Computer Methods in Applied Mechanics and Engineering*, 139:289–314, 1996.

[6] I. Babuska and J.M. Melenk. The partition of unity method. *International Journal for Numerical Methods in Engineering*, 40(4):727–758, 1997.

[7] M.S. Mohamed, O. Laghrouche, and A. El-Kacimi. Some numerical aspects of the pufem for efficient solution of 2d helmholtz problems. *Computers and Structures*, 88:1484–1491, 2010.

[8] O. Laghrouche and M.S. Mohamed. Locally enriched finite elements for the helmholtz equation in two dimensions. *Computers and Structures*, 88:1469–1473, 2010.

[9] O. Laghrouche, P. Bettess, E. Perrey-Debain, and J. Trevelyan. Wave interpolation finite elements for helmholtz problems with jumps in the wave speed. *Computer Methods in Applied Mechanics and Engineering*, 194:367–381, 2005.

[10] A. El Kacimi and O. Laghrouche. Numerical modelling of elastic wave scattering in frequency domain by the partition of unity finite element method. *International Journal for Numerical Methods in Engineering*, 77(12):1646–1669, 2009.

[11] A. El Kacimi and O. Laghrouche. Improvement of pufem for the numerical solution of high-frequency elastic wave scattering on unstructured triangular mesh grids. *International Journal for Numerical Methods in Engineering*, 84(3):330–350, 2010.

[12] J.-D. Chazot, B. Nennig, and E. Perrey-Debain. Performances of the partition of unity finite element method for the analysis of two-dimensional interior sound fields with absorbing materials. *Journal of Sound and Vibration*, 332(8):1918–1929, 2013.

[13] J.-D. Chazot, E. Perrey-Debain, and B. Nennig. The partition of unity finite element method for the simulation of waves in air and poroelastic media. *Journal of the Acoustical Society of America*, 135(2):724–733, 2014.

[14] M. Yang, E. Perrey-Debain, B. Nennig, and J.-D. Chazot. Development of 3d pufem with linear tetrahedral elements for the simulation of acoustic waves in enclosed cavities. *Computer Methods in Applied Mechanics and Engineering*, 335:403 – 418, 2018.

[15] I. Babuška and Z. Zhang. The partition of unity method for the elastically supported beam. *Computer Methods in Applied Mechanics and Engineering*, 152(1):1 – 18, 1998. Containing papers presented at the Symposium on Advances in Computational Mechanics.

[16] M. Arndt, R. D. Machado, and A. Scremin. The generalized finite element method applied to free vibration of beams. *Proceedings of COBEM 2009, Brazil*, 2009.

[17] M. Arndt, R.D. Machado, and A. Scremin. The generalized finite element method applied to free vibration of framed structures. In *Advances in Vibration Analysis Research*. InTech, 2011.

[18] Y.S. Hsu. Enriched finite element methods for timoshenko beam free vibration analysis. *Applied Mathematical Modelling*, 40(15):7012 – 7033, 2016.

[19] R.R. Craig. *Structural dynamics: an introduction to computer methods*. Wiley New York, 1981.

[20] L. Hazard and P. Bouillard. Structural dynamics of viscoelastic sandwich plates by the partition of unity finite element method. *Computer Methods in Applied Mechanics and Engineering*, 196(41):4101 – 4116, 2007.

[21] E. De Bel, P. Villon, and P. Bouillard. Forced vibrations in the medium frequency range solved by a partition of unity method with local information. *International Journal for Numerical Methods in Engineering*, 62(9):1105–1126, 2005.

[22] S.M. Hashemi, M.J. Richard, and G. Dhatt. A new dynamic finite element (dfe) formulation for lateral free vibrations of euler–bernoulli spinning beams using trigonometric shape functions. *Journal of Sound and Vibration*, 220(4):601–624, 1999.

[23] J.-L. Guyader. *Vibration in Continuous Media*. ISTE Ltd, 2006.

[24] A.W. Leissa and M.S. Qatu. *Vibrations of Continuous Systems.* McGraw-Hill, 2011.

[25] T.J. Hughes, R.L. Taylor, and W. Kanoknukulchai. A simple and efficient finite element for plate bending. *International Journal for Numerical Methods in Engineering*, 11(10):1529–1543, 1977.

[26] M. Petyt. *Introduction to finite element vibration analysis*. Cambridge university press, 2010.

[27] H. Bang and Y.W. Kwon. *The finite element method using MATLAB*. CRC press, 2000.

[28] D.L. Thomas, J.M. Wilson, and R.R. Wilson. Timoshenko beam finite elements. *Journal of Sound and Vibration*, 31(3):315 – 330, 1973.

[29] J.S. Przemieniecki. *Theory of matrix structural analysis*. New York: McGraw-Hill, 1968.

[30] A. Tveito and R. Winther. *Introduction to partial differential equations: a computational approach*, volume 29. Springer Science & Business Media, 2004.

[31] E. Perrey-Debain, J. Trevelyan, and P. Bettess. Plane wave interpolation in direct collocation boundary element method for radiation and wave scattering: numerical aspects and applications. *Journal of sound and vibration*, 261(5):839–858, 2003.

[32] O. Beslin and J. Nicolas. A hierarchical functions set for predicting very high order plate bending modes with any boundary conditions. *Journal of sound and vibration*, 202(5):633–655, 1997.

[33] G.R. Bhashyam and G. Prathap. The second frequency spectrum of timoshenko beams. *Journal of Sound and Vibration*, 76(3):407–420, 1981.

[34] R. Davis, R.D. Henshell, and G.B. Warburton. A timoshenko beam element. *Journal of Sound and Vibration*, 22(4):475–487, 1972.

[35] S. Corn, N. Bouhaddi, and J. Piranda. Transverse vibrations of short beams: Finite element models obtained by a condensation method. *Journal of Sound and Vibration*, 201(3):353 – 363, 1997.

[36] A.W. Lees and D.L. Thomas. Unified timoshenko beam finite element. *Journal of Sound and Vibration*, 80(3):355 – 366, 1982.

Appendix A

Linear element

The stiffness matrix of the classical linear element using exact integrations has the form

$$\mathbb{K}_e = \frac{EI}{l_e^3\phi}\begin{bmatrix} 12 & -6l_e & -12 & -6l_e \\ & l_e^2(4+\phi) & 6l_e & l_e^2(2-\phi) \\ & & 12 & 6l_e \\ & \text{sym.} & & l_e^2(4+\phi) \end{bmatrix}, \tag{15}$$

with $\phi = 12EI/G\kappa Sl_e^2$. This formulation is known to suffer from shear-locking effects and a reduced integration technique is usually employed [26], this gives

$$\mathbb{K}_e = \frac{EI}{l_e^3\phi}\begin{bmatrix} 12 & -6l_e & -12 & -6l_e \\ & l_e^2(3+\phi) & 6l_e & l_e^2(3-\phi) \\ & & 12 & 6l_e \\ & \text{sym.} & & l_e^2(3+\phi) \end{bmatrix}, \tag{16}$$

More details of the stiffness matrix can be found Refs. [25, 26, 27] (here some signs can change depending on the convention for the rotation angle). The associated mass matrix is

$$\mathbb{M}_e = \rho S l_e \begin{bmatrix} 1/3 & 0 & 1/6 & 0 \\ & r^2/3 & 0 & r^2/6 \\ & & 1/3 & 0 \\ & \text{sym.} & & r^2/3 \end{bmatrix}, \tag{17}$$

where $r = \sqrt{I/S}$ is the radius of gyration. This matrix can also be found with more details in Refs. [33, 26]. Note the differences between the two resulting stiffness matrices appears in the components $\mathbb{K}_{22}$, $\mathbb{K}_{24}$, $\mathbb{K}_{42}$ and $\mathbb{K}_{44}$. This difference is due to the different integration points adopted for evaluating the shear modulus matrix. When using exact integrations, the shear locking effects appear for the cases where the Euler-Bernoulli or thin beam model is applicable. The shear-locking effects can be overcome by h-refinement, which makes the stiffness matrix obtained by exact and reduced integrations consistent.

Enhanced element

A specific timoshenko beam element is also often used to solve beam problems in the litterature [29, 26, 34, 28, 35, 36]. This enhanced element is based on a cubic and a quadratic interpolation for the transverse displacement w and the rotation β, respectively, with an added constraint between w and β in order to satisfy the static equilibrium equation. The shape functions $\hat{N}_i$ in Eq. (13) are given below

$$\hat{N}_1 = \frac{1}{1+\phi}\left[1+\phi-\phi\xi-3\xi^2+2\xi^3\right], \quad \hat{N}_2 = \frac{l_e/2}{1+\phi}\left[(2+\phi)\xi-(4+\phi)\xi^2+2\xi^3\right],$$
$$\hat{N}_3 = \frac{1}{1+\phi}\left[\phi\xi+3\xi^2-2\xi^3\right], \quad \hat{N}_4 = \frac{l_e/2}{1+\phi}\left[-\phi\xi-(2-\phi)\xi^2+2\xi^3\right],$$
$$\hat{N}_5 = \frac{2/l_e}{1+\phi}\left[-3\xi+3\xi^2\right], \quad \hat{N}_6 = \frac{1}{1+\phi}\left[1+\phi-(4+\phi)\xi+3\xi^2\right],$$
$$\hat{N}_7 = \frac{2/l_e}{1+\phi}\left[3\xi-3\xi^2\right], \quad \hat{N}_8 = \frac{1}{1+\phi}\left[-(2-\phi)\xi+3\xi^2\right],$$

with $\phi = 12EI/G\kappa Sl_e^2$. The resultant stifness matrix remains of the same size as they correpond to nodal values and

$$\mathbb{K}_e = \frac{EI}{l_e^3(1+\phi)}\begin{bmatrix} 12 & -6l_e & -12 & -6l_e \\ & l_e^2(4+\phi) & 6l_e & l_e^2(2-\phi) \\ & & 12 & 6l_e \\ & \text{sym.} & & l_e^2(4+\phi) \end{bmatrix}. \tag{18}$$

This matrix can be found with all necessary details in [28, 29, 26]. This enhanced element is also free of shear locking. The the mass matrix writes :

$$\mathbb{M}_e = \frac{\rho S l_e}{(1+\phi)^2} \begin{bmatrix} m_1 & -m_2 & m_3 & -m_4 \\ & m_5 & m_4 & m_6 \\ & & m_1 & m_2 \\ \text{sym.} & & & m_5 \end{bmatrix} + \frac{\rho S l_e}{(1+\phi)^2} \left(\frac{r}{l_e}\right)^2 \begin{bmatrix} m_7 & -m_8 & -m_7 & -m_8 \\ & m_9 & m_8 & m_{10} \\ & & m_7 & m_8 \\ \text{sym.} & & & m_9 \end{bmatrix}, \tag{19}$$

where coefficients m_i are given below and this mass matrix can also be found with more details in Refs. [28, 29, 26].

$$\begin{aligned}
m_1 &= \frac{13}{35} + \frac{7\phi}{10} + \frac{\phi^2}{3} \quad , & m_2 &= \left(\frac{11}{210} + \frac{11\phi}{120} + \frac{\phi^2}{24}\right) l_e \quad , \\
m_3 &= \frac{9}{70} + \frac{3\phi}{10} + \frac{\phi^2}{6} \quad , & m_4 &= -\left(\frac{13}{420} + \frac{3\phi}{40} + \frac{\phi^2}{24}\right) l_e \quad , \\
m_5 &= \left(\frac{1}{105} + \frac{\phi}{60} + \frac{\phi^2}{120}\right) l_e^2 \quad , & m_6 &= -\left(\frac{1}{140} + \frac{\phi}{60} + \frac{\phi^2}{120}\right) l_e^2 \quad , \\
m_7 &= \frac{6}{5} \quad , & m_8 &= \left(\frac{1}{10} - \frac{\phi}{2}\right) l_e \quad , \\
m_9 &= \left(\frac{2}{15} + \frac{\phi}{6} + \frac{\phi^2}{3}\right) l_e^2 \quad , & m_{10} &= \left(-\frac{1}{30} - \frac{\phi}{6} + \frac{\phi^2}{6}\right) l_e^2 \quad .
\end{aligned}$$